Article

Flexibility Optimization in Robust Co-Optimization of Combined Power System and Gas Networks Using Transmission Lines' Switching

Mohammad Ghasemloo, Maryam A. Hejazi * and **Hamed Hashemi-Dezaki**

Department of Electrical and Computer Engineering, University of Kashan, 6 km Ghotbravandi Blvd, Kashan 8731753153, Iran
* Correspondence: mhejazi@kashanu.ac.ir; Tel.: +98-31-5591-3483

Abstract: The operational flexibility in electricity networks with a high penetration rate of renewable resources has received a great deal of attention. In several research works, gas network constraints have been studied in operational flexibility studies because specific characteristics of the gas-fired units play a major role in procuring flexibility. However, the literature shows that the interval range of the uncertainty set has been assumed to be deterministic in most of the available research works. This paper tries to fill the research gap about stochastic modeling of the interval range of the uncertainty set. It considers the uncertainty set's interval range an uncertain parameter, allowing optimal scheduling with less conservative assumptions. In addition, transmission lines' switching is considered to optimize the network topology when the N-1 reliability measure is adopted. As a nonconvex problem, the recourse decision level would be a mixed-integer program (MIP), for which an exact nested column-and-constraint generation algorithm is used to find the best solutions. The proposed method was applied to IEEE six-bus and 39-bus test systems, interconnecting their corresponding gas networks. The test results infer that in a specified risk level for the IEEE six-bus and 39-bus test systems, with a rather slight increase (7.3% and 065%) in the operation cost, a large reduction (89% and 99%) in the out-of-sample cost could be obtained, respectively. The test results illustrate the advantages of the proposed method, using the variable interval range of the uncertainty set and corrective transmission lines' switching. In addition, it was shown that if transmission switching is not considered, the total cost rises up to 18.8%.

Keywords: operational flexibility; reliability constrained co-optimization scheduling; combined electricity and gas networks; corrective switching of transmission lines; nested column-and-constraint generation (CCG) algorithm

1. Introduction

Nowadays, the deployment of gas-fired generators (GFGs) is an effective alternative for governments and system operators. GFGs specifications, e.g., high ramp rates, economic aspects, and fast start-up/shut-down, emphasize their effectiveness [1,2]. These units are well suited to the uncertain and variable nature of renewable energy sources (RES) [3–5]. However, the functionality and availability of gas units depend highly on the gas network status [6,7]. Low pressure and congested pipelines restrict the applicability of GFGs to respond appropriately [8,9].

Most research works in the literature have focused on the interconnection of electricity and natural gas networks [10–12]. In [13], a two-stage profit maximization problem has been proposed, including electricity and natural gas markets. The locational marginal prices were optimized in the inner market-clearing stage, while all players could access equilibrium to guarantee their maximum profit at the outer level. The GFGs and gas market were jointed through bids from GFGs and prices in the gas market in [13]. Chen et al. [14] reported a new study to handle congestions in gas networks properly. A comprehensive,

interconnected electricity and gas network operational scheduling problem in a market-based model has been proposed by Chen et al. [14], where gas transmission capacity was labeled with a certain price. Additionally, RES uncertainties were considered. In [15], gas storages were adopted to smooth out the load profile embedded in the robust operation for interconnected electricity and natural gas networks, where the robustness was against multiple component outages. In addition, a relaxed second-order conic programming (SOC) form of gas network constraints was considered in a decomposition-based algorithm called column and constraint generation (CCG). The uncertainties regarding electricity and gas demand have been investigated in both electricity and gas networks by the introduced distributionally robust scheduling problem in [16]. To linearize nonconvexities regarding gas network operation, the problem has been converted into mixed-integer linear programming (MILP), benefiting approximated linear decision rules to deal with uncertainties by He et al. [16]. In [17], for the sake of a more tractable solution of computational complexity and reducing the requirements of heavy communication facilities, fully decentralized combined electricity and gas network operational planning was developed. He et al. [17] adopted the iterative alternating direction method of multipliers (I-ADMM) to convexify nonconvex constraints regarding gas networks. In [18], for a mutual electricity and gas network operational planning problem, the potential advantages of using power-to-gas (P2G) storage have been assessed on a day-ahead basis to make gas consumption more affordable. In [19], energy procurement cost minimization has been focused on considering three different types of uncertainties, e.g., distributed energy resources (DER), day-ahead electric demand, and natural gas demand profiles, in a joint gas and electricity schedule. Two-stage robust optimization was applied by Chen et al. [19].

Transmission line switching to maximize system flexibility and other optimal operation features is also considered in recent research [20–22]. Due to the increased tendency to maximize the penetration rate of RES in future networks and more requirements for additional network flexibility to tackle possible congestions on one side and deal with system reliability on the other side, optimal transmission line switching would be a key solution in the viewpoint of flexibility in the transmission side. Reference [23] is one of the most recent research works in the field of power system flexibility maximization. In [23], optimal transmission line switching (TS) has been investigated in a contingency-constrained unit commitment through a robust optimization approach in both preventive and corrective modes.

In Table 1, the literature review is summarized. The features and factors of the comparative literature review could be listed as follows:

Factor 1: Combined electricity and gas networks operational planning;
Factor 2: Considering optimal transmission line switching;
Factor 3: Common uncertainty resources related to the electrical system, e.g., renewable sources' output power or demand uncertainties;
Factor 4: Nonlinearities of gas network constraints;
Factor 5: Flexibility reserve deployment;
Factor 6: Decision making based on robust optimization; and
Factor 7: Considering the uncertainty set's interval range as an uncertain parameter.

The literature review illustrates the research gap in stochastic modeling of the uncertainty set's interval range. In the proposed method, unlike in existing robust optimization methods, dealing with uncertainties by introducing uncertainty sets with respective pre-defined ranges, adjustable interval ranges as an additional degree of freedom to prevent conservativeness of the robust optimizations are considered. Moreover, the studies of TS, as one of the most effective preventive and corrective solutions to maximize system flexibility, have received less attention. The main contributions of this article are proposed to fill such research gaps. Considering the detailed nonlinear constraints of the gas network is another minor contribution.

Table 1. Comparative summary of the literature review in the field of flexibility maximization of interconnected electric and gas networks.

Ref. No.	Factor 1	Factor 2	Factor 3	Factor 4	Factor 5	Factor 6	Factor 7
[13]	✓	–	–	–	–	–	–
[14]	✓	–	✓	–	–	–	–
[15]	✓	–	–	–	✓	✓	–
[16]	✓	–	✓	✓	✓	✓	–
[17]	✓	–	–	–	–	–	–
[18]	✓	–	–	–	–	–	–
[19]	✓	–	✓	–	✓	✓	–
[24]	✓	–	–	–	✓	✓	–
[25]	✓	–	–	–	–	–	–
[23]	–	✓	–	–	–	✓	–
Proposed model	✓	✓	✓	✓	✓	✓	✓

This paper tries to fill existing gaps in the literature about the flexibility maximization of interconnected electric and gas networks. The main contributions of this article can be listed as follows:

- This research majorly focuses on flexibility maximization through the respective uncertain range in a multistage robust optimization approach to reach less conservativeness. This is one of the major contributions. Modeling an uncertain interval range is a new framework that is proposed in this paper. It should be highlighted that Factor 7 has been used in this article as a new method, considering the uncertainty set's interval range as an uncertain parameter.

- In this paper, the reported method of [23] would be extended, while TS is considered in a joint robust security-constrained unit commitment and nonlinear gas network scheduling problem. Using TS in co-optimization of combined gas and electricity networks, besides other robust security-constrained unit commitment issues, is one of the contributions.

- A three-level model is developed for the joint robust security constraint unit commitment (SCUC) and gas network scheduling. In the upper minimization level, a base SCUC is solved, considering nonlinear gas network constraints aiming to minimize operational cost without considering explicit uncertainties. In the middle maximization problem, the worst possible scenario for uncertain parameters corresponding to RES output power and the most critical electric transmission line outage are concerned. In the lower minimization re-dispatch problem, the model tries to cover the worst cases found in the previous level with the lowest re-dispatch cost. The proposed three-level optimization model, besides other new aspects, can be listed as one of the contributions. However, separate three-level models might be introduced in the available works.

- The nonlinearity of gas network constraints and integer decision variables regarding corrective optimal TS makes robust optimization challenging. The inner optimization levels consist of nonlinear and integer terms, which is not compatible with strong duality theory. Accordingly, a state-of-the-art nested column and constraint generation (CCG) method is applied to overcome this challenge [26].

The proposed method has tried to respond to all concerns comprehensively. Indeed, one of the main advantages of this study and the proposed model is its consideration of all aspects. However, it is necessary to clarify how the proposed model can consider various aspects, and related challenges should be highlighted. Developing a three-level optimization model is one of the solutions that can overcome some complexities in the proposed model. Indeed, by a three-level model, the optimization problem can be solved more easily. In addition, TS is another solution that has been utilized to satisfy the constraints of the optimization problem. TS can also be useful in a realistic situation. Furthermore,

linearized techniques and some innovative approaches to solving the optimization problem are other features of this research. These capabilities help use the proposed method in realistic systems.

The remainder of this article's structure is as follows. Section 2 is (Uncertain Interval Range Modeling) allocated for the introduced multistage robust gas network constrained (GC)-SCUC optimization problem. A brief nested CCG counterpart of the proposed GC-SCUC model (Problem Formulation) is reported in Section 3. Section 4 presents the test and numerical results. Finally, the conclusion is given in Section 5.

2. Adjustable Interval Range Modeling to Consider Stochastic Behaviors and Uncertainties

In existing references, the interval/respective range has been assumed to be deterministic, which has fixed endpoints in both up and down directions. The interval range could be distinguished according to recorded/measured data and statistical analyses for the stochastic subsystems based on selected confidence interval (CI) levels. Unlike the available studies based on a fixed interval range, e.g., ± 10 or $\pm 20\%$ of the predicted/estimated parameter, this paper considers a stochastic-based interval for uncertain subsystems/elements. By modeling the stochastic behaviors of the interval range, the introduced framework searches corresponding to the worst scenario, while conservative decision making can be reduced, and more precision deviations in stochastic subsystems between two consecutive intervals are achievable. The concept of the variable interval range is depicted in Figure 1. Figure 1 shows a conceptual net load variation, besides the predicted values and up/down deviations with various CIs.
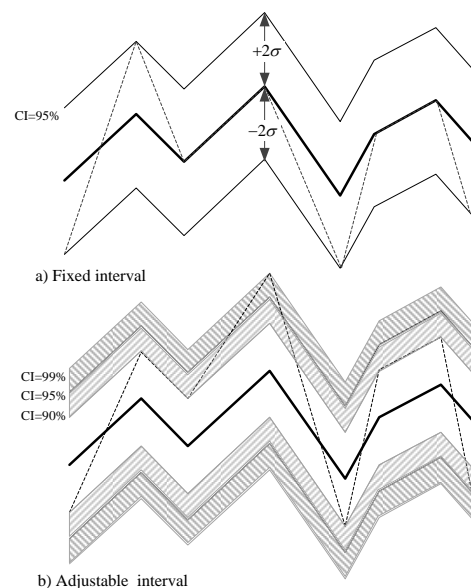

Figure 1. Conceptual overview of the flexible/adjustable interval range. (**a**) Fixed and (**b**) adjustable.

As revealed in Figure 1b, a flexible confidence interval of 95% is considered for up/down directions. From the statistical point of view, the interval range could deviate in various intervals of the operational conditions for a CI between 90 and 99%.

Moreover, deviations of the stochastic parameters in several intervals could be kept in a smaller range, which leads to lower conservativeness. Furthermore, larger deviations between consecutive intervals are plausible with the developed stochastic adjustable interval range, resulting in more intertemporal flexibility. The introduced new uncertainty set

development is described according to Equations (1)–(3) for the net load (one of the most important stochastic parameters in the operation of electrical energy systems).

$$S.t.\ ND_{n,t} = L_{n,t} + \Delta N_{n,t}^u z_{n,t}^u - \Delta N_{n,t}^d z_{n,t}^d$$
$$\forall n \in \Lambda, t \in T \tag{1}$$

$$\Delta N_{n,t}^u = \Delta N_{n,t}^{u0} + \Delta N_{n,t}^{u+} z_{n,t}^{u+} - \Delta N_{n,t}^{u-} z_{n,t}^{u-} \tag{2}$$

$$\Delta N_{n,t}^d = \Delta N_{n,t}^{d0} + \Delta N_{n,t}^{d+} z_{n,t}^{d+} - \Delta N_{n,t}^{d-} z_{n,t}^{d-} \tag{3}$$

In Equation (1), the net load uncertainty for the *n*-th bus at the *t*-th time period is mathematically expressed based on two binary/Boolean variables that permit deviations around the predicted/estimated value with a predetermined fixed interval range. In the introduced formulation, asymmetric and flexible/adjustable interval ranges are assumed for both up/down changes. By applying Equations (2) and (3), Equations (1) and (4) can be expressed according to multiplied binary values. The linearizing of nonlinear parts can be implemented by the Big-M technique and the dummy variables, as shown in Equations (4)–(12).

$$ND_{n,t} = L_{n,t} + \Delta N_{n,t}^{u0} z_{n,t}^u + \Delta N_{n,t}^{u+} \underbrace{z_{n,t}^{u+} z_{n,t}^u}_{U_{n,t}^+} - \Delta N_{n,t}^{u-} \underbrace{z_{n,t}^{u-} z_{n,t}^u}_{U_{n,t}^-}$$
$$- \Delta N_{n,t}^{d0} z_{n,t}^d + \Delta N_{n,t}^{d+} \underbrace{z_{n,t}^{d+} z_{n,t}^d}_{D_{n,t}^+} - \Delta N_{n,t}^{u-} \underbrace{z_{n,t}^{d-} z_{n,t}^d}_{D_{n,t}^-} \tag{4}$$
$$\forall n \in \Lambda, t \in T$$

$$- M z_{n,t}^{u+} \le U_{n,t}^+ \le M z_{n,t}^{u+} \tag{5}$$

$$z_{n,t}^u - M(1 - z_{n,t}^{u+}) \le U_{n,t}^+ \le z_{n,t}^u + M(1 - z_{n,t}^{u+}) \tag{6}$$

$$- M z_{n,t}^{u-} \le U_{n,t}^- \le M z_{n,t}^{u-} \tag{7}$$

$$z_{n,t}^u - M(1 - z_{n,t}^{u-}) \le U_{n,t}^- \le z_{n,t}^u + M(1 - z_{n,t}^{u-}) \tag{8}$$

$$- M z_{n,t}^{d+} \le D_{n,t}^+ \le M z_{n,t}^{d+} \tag{9}$$

$$z_{n,t}^d - M(1 - z_{n,t}^{d+}) \le D_{n,t}^+ \le z_{n,t}^d + M(1 - z_{n,t}^{d+}) \tag{10}$$

$$- M z_{n,t}^{d-} \le D_{n,t}^- \le M z_{n,t}^{d-} \tag{11}$$

$$z_{n,t}^d - M(1 - z_{n,t}^{d-}) \le D_{n,t}^- \le z_{n,t}^d + M(1 - z_{n,t}^{d-}) \tag{12}$$

Inequality Equations (13)–(16) should be considered to represent that the binary variables of the stochastic interval range depend on those of the stochastic net load.

$$z_{n,t}^{u+} \le z_{n,t}^u \tag{13}$$

$$z_{n,t}^{u-} \le z_{n,t}^u \tag{14}$$

$$z_{n,t}^{d+} \le z_{n,t}^d \tag{15}$$

$$z_{n,t}^{d-} \le z_{n,t}^d \tag{16}$$

The simultaneous up and down deviations in stochastic elements that are not possible are modeled by Equations (17)–(19).

$$z_{n,t}^u + z_{n,t}^d \le 1 \quad \forall n \in \Lambda,\ t \in T \tag{17}$$

$$z_{n,t}^{u+} + z_{n,t}^{u-} \le 1 \quad \forall n \in \Lambda,\ t \in T \tag{18}$$

$$z_{n,t}^{d+} + z_{n,t}^{d-} \leq 1 \quad \forall n \in \Lambda, \ t \in \mathrm{T} \tag{19}$$

Finally, the budget of uncertainties is defined as Equations (20)–(22) to control the conservativeness of the extreme points.

$$\sum_{n \in \Lambda} \sum_{t \in \mathrm{T}} z_{n,t}^{u} + z_{n,t}^{d} \leq \Gamma \tag{20}$$

$$\sum_{n \in \Lambda} \sum_{t \in \mathrm{T}} z_{n,t}^{u+} + z_{n,t}^{u-} \leq \Gamma^{u} \tag{21}$$

$$\sum_{n \in \Lambda} \sum_{t \in \mathrm{T}} z_{n,t}^{d+} + z_{n,t}^{d-} \leq \Gamma^{d} \tag{22}$$

3. Problem Formulation

The introduced tri-level min-max-min robust model/concept for the joint electricity and natural gas SCUC optimization problem is discussed in this part. Afterward, the methodology based on the nested CCG solution is presented.

This section may be divided into subheadings. It should provide a concise and precise description of the experimental results, their interpretation, as well as the experimental conclusions that can be drawn.

3.1. Proposed Robust SCUC Problem

The main goal of this paper is to co-optimally schedule day-ahead electricity and natural gas networks based on flexibility optimization using a flexible/adjustable interval range and switching of transmission lines as decision variables of the optimization problem. Hence, a robust tri-level SCUC is developed. The SCUC should be solved, as one of the first steps, in the introduced robust tri-level SCUS for the base case, while uncertain resources are neglected. The scenarios based on worth conditions for both uncertain net load and the worst possible transmission line contingency are distinguished by finding the maximum solutions in the middle level. Finally, at the inner level, units with flexibility capabilities are re-dispatched, which is the selected solution for decision making in both electricity and natural gas networks.

The objective function, as shown in Equation (23), is presented for cost terms, including the costs for TG's start-up, no-load, energy generation, and the up/down reserve capacity allocation. In addition, cost terms related to gas production out of gas wells and gas storing costs are considered in the proposed objective function. The start-up costs, no-load cost functions, and power production from GFGs are also considered to determine the introduced objective function. Furthermore, the up and down reserve capacity costs of GFGs are considered.

The power balance based on predicted/estimated net load is depicted in Equation (24). In addition, the nodal power balance according to shift factor sensitivity matrices is considered in the model by Equation (25). The up and down reserve capacity allocations for GFGs are restricted by maximum and minimum generation capacity, as given in Equations (26) and (27), respectively [27,28]. Similarly, Equations (28) and (29) are used to limit TGs' capacity from the viewpoint of generation and reserve. The GFGs and TGs' reserve capacities should be controlled and re-dispatched to reach the desired capacities, as expressed in Equations (30)–(33). The minimum and maximum gas production out of a gas well are represented by Equation (34) [29]. The time-dependent rate for storing gas is embedded in Equation (35), while this rate is restricted according to Equation (36). The maximum gas storage in and out ranges of a gas storage unit is limited in Equations (37) and (38), respectively. As shown in Equation (39), the gas pressure limit at each node should be considered in the proposed optimization problem. The gas balance requirement is presented in Equation (40).

$$\text{Min} \sum_{t=1}^{T} \left\{ \sum_{i \in \Omega^{\text{Tr}}} \left(C_i^{\text{Tr,SU}} + x_{i,t} C_i^{\text{Tr,NL}} + c_i^{\text{Tr}} P_{i,t}^{\text{Tr}} \right. \right.$$
$$\left. + USC_i^{\text{Tr}} SP_{i,t}^{\text{Tru}} + DSC_i^{\text{Tr}} SP_{i,t}^{\text{Trd}} \right) + \sum_{w \in W} Q_w q_{wt} + \sum_{s \in S} Q_s q_{st}$$
$$\left. + \sum_{g \in \Omega^{\text{G}}} \left(C_g^{\text{G,SU}} + x_{g,t} C_g^{\text{G,NL}} + c_g^{\text{G}} P_{g,t}^{\text{G}} + USC_g^{\text{G}} SP_{g,t}^{\text{Gu}} + DSC_g^{\text{G}} SP_{g,t}^{\text{Gd}} \right) \right\} \tag{23}$$

$$\sum_{i \in \Omega^{\text{Tr}}} P_{i,t}^{\text{Tr}} + \sum_{g \in \Omega^{\text{G}}} P_{g,t}^{\text{G}} = \sum_{n \in \Lambda} NL_{n,t} \ \forall t \in T \tag{24}$$

$$-F_l^{\max} \leq \sum_{n \in \Lambda} SF_{n,l} \left(\sum_{i \in \Omega_n^{\text{Tr}}} P_{i,t}^{\text{Tr}} + \sum_{g \in \Omega_n^{\text{G}}} P_{g,t}^{\text{G}} - NL_{n,t} \right) \leq F_l^{\max} \forall l \in \text{NL}, t \in T \tag{25}$$

$$P_{g,t}^{\text{G}} + SP_{g,t}^{\text{Gu}} \leq x_{g,t} P_g^{\text{G,max}} \quad \forall g \in \Omega^{\text{G}}, t \in T \tag{26}$$

$$P_{g,t}^{\text{G}} - SP_{g,t}^{\text{Gd}} \geq x_{g,t} P_g^{\text{G,min}} \quad \forall g \in \Omega^{\text{G}}, t \in T \tag{27}$$

$$P_{i,t}^{\text{Tr}} + SP_{i,t}^{\text{Tru}} \leq x_{i,t} P_i^{\text{Tr,max}} \quad \forall i \in \Omega^{\text{Tr}}, t \in T \tag{28}$$

$$P_{i,t}^{\text{Tr}} - SP_{i,t}^{\text{Trd}} \geq x_{i,t} P_i^{\text{Tr,min}} \quad \forall i \in \Omega^{\text{Tr}}, t \in T \tag{29}$$

$$0 \leq SP_{g,t}^{\text{Gu}} \leq R_g^{\text{Gu,max}} \quad \forall g \in \Omega^{\text{G}}, t \in T \tag{30}$$

$$0 \leq SP_{g,t}^{\text{Gd}} \leq R_g^{\text{Gd,max}} \quad \forall g \in \Omega^{\text{G}}, t \in T \tag{31}$$

$$0 \leq SP_{i,t}^{\text{Tru}} \leq R_i^{\text{Tru,max}} \quad \forall i \in \Omega^{\text{Tr}}, t \in T \tag{32}$$

$$0 \leq SP_{i,t}^{\text{Trd}} \leq R_i^{\text{Trd,max}} \quad \forall i \in \Omega^{\text{Tr}}, t \in T \tag{33}$$

$$q_w^l \leq q_{wt} \leq q_w^u \tag{34}$$

$$r_{st} = r_{s,t-1} + q_{st}^{in} - q_{st}^{out} \tag{35}$$

$$r_s^l \leq r_{st} \leq r_s^u \tag{36}$$

$$0 \leq q_{st}^{in} \leq q_{s,max}^{in} \tag{37}$$

$$0 \leq q_{st}^{out} \leq q_{s,max}^{out} \tag{38}$$

$$\left(\tau_j^l \right)^2 \leq v_{jt} \leq \left(\tau_j^u \right)^2 \tag{39}$$

$$\sum_{j' \in \phi_J(j)} (q_{jj',t}^{out} - q_{jj',t}^{in}) + \sum_{s \in \phi_S(j)} (q_{st}^{out} - q_{st}^{in}) + \sum_{w \in \phi_w(j)} q_{wt} - \sum_{e \in \phi_e(j)} q_{et} - \sum_{g \in \phi_{\Omega^{\text{G}}}(j)} b_g P_{g,t}^{\text{G}} = 0 \tag{40}$$

In Equation (41), the nonlinear Weymouth equation [30,31] shows the relationship between gas flow in the *y*-th pipeline and the start and end node gas pressure. This equation could be linearized using Equations (42)–(45).

$$q_{yt} |q_{yt}| = \psi_y (v_{i1t} - v_{j2t}) \tag{41}$$

$$\theta(q_{yt}) \approx \theta(\Delta_{yt}^0) + \sum_{k \in K} \left(\theta(\Delta_{yt}^{k+1}) - \theta(\Delta_{yt}^k) \right) v_{ytk} \tag{42}$$

$$q_{yt} = \Delta_{yt}^0 + \sum_{k \in K} \left(\Delta_{yt}^{k+1} - \Delta_{yt}^k \right) v_{ytk} \tag{43}$$

$$v_{ytk+1} \leq \vartheta_{ytk} \leq v_{ytk} \ \forall k \in K - 1 \tag{44}$$

$$0 \leq v_{ytk} \leq 1 \ \forall k \in K \tag{45}$$

where $\theta(q_{yt})$ represents a nonlinear term $q_{yt}|q_{yt}|$ in Equation (41). In addition, Δ_{yt}^k are piecewise segments of the nonlinear term. In Equations (42)–(45), v_{ytk} and ϑ_{ytk} are auxiliary continuous and binary variables, respectively. The error gap could be controlled by choosing different sizes of the K value as piecewise linear partitions.

The coefficient ψ_y, as used in Equation (41), is defined in Equation (46). The gas pressure in the pipeline endpoints equipped with a compressor, known as an active line, is indicated in Equation (47). The gas flow in the active pipelines is shown in Equation (48). The start-up costs of TGs and GFGs are calculated using Equations (49)–(52). A set of constraints representing the minimum up/down-time constraints for all types of generation units is defined in Equation (53). For the space-saving purpose, these constraints have been discussed in brief form, and detailed formulations and supplementary explanations can be found in [32].

$$\psi_y = \frac{\pi^2\lambda^2 R_y^5}{16 Line_y F_y \mu Temp Z_y \rho_0^2} \tag{46}$$

$$v_{j2} \le \gamma_c^2 b_c v_{j1} + (1 - b_c)(\tau_{j2}^u)^2 \tag{47}$$

$$0 \le q_{ct} \le M b_c \tag{48}$$

$$C_i^{\text{Tr,SU}} \ge SC_i^{\text{Tr}}(x_{i,t} - x_{i,t-1}) \quad \forall i \in \Omega^{\text{Tr}} \tag{49}$$

$$C_i^{\text{T,SU}} \ge 0 \quad \forall i \in \Omega^{\text{T}} \tag{50}$$

$$C_g^{\text{G,SU}} \ge SC_g^{\text{G}}(x_{g,t} - x_{g,t-1}) \quad \forall g \in \Omega^{\text{G}} \tag{51}$$

$$C_g^{\text{G,SU}} \ge 0 \quad \forall g \in \Omega^{\text{G}} \tag{52}$$

$$\mathbf{\kappa_{i/g}} \in \{0,1\} \cap \mathbf{k_{i/g}} \quad \forall i \in \Omega^{\text{Tr}}, g \in \Omega^{\text{G}}, \ t \in \text{T} \tag{53}$$

The mathematical expression of the middle maximization level is presented in Equations (54)–(58). The middle maximization level has been developed to determine the worst scenarios from the viewpoint of stochastic behaviors of net load and transmission line contingency. The maximum of allowed contingencies is restricted according to Equation (58). The set of uncertain and stochastic parameters in the developed robust optimization problem will be polyhedral. The introduced model is linearized utilizing auxiliary binary variables [33]. Unlike the available studies, a flexible/adjustable interval range will be utilized to search for a wider range of flexibility in the power system operation.

$$\Phi^{wc} = 0 \tag{54}$$

$$\Phi^{wc} = \text{Max } \Phi \tag{55}$$

$$S.t. \ ND_{n,t} = L_{n,t} + \Delta N_{n,t}^{u0} z_{n,t}^u - \Delta N_{n,t}^{d0} z_{n,t}^d + \Delta_{n,t}^{u+} U_{n,t}^+$$
$$- \Delta_{n,t}^{u-} U_{n,t}^- - \Delta_{n,t}^{d+} D_{n,t}^+ + \Delta_{n,t}^{d-} D_{n,t}^- \tag{56}$$
$$\forall n \in \Lambda, \ t \in \text{T}$$

$$(5) \text{ to } (22) \tag{57}$$

$$\sum_{l \in NL} a_{lt} \ge NL - 1 \ \forall t \in \text{T} \tag{58}$$

As demonstrated by Equations (59)–(76), the lower minimization level would be a recourse decision-making problem (mixed-integer problem). At the lower minimization level, the commitment of the units does not change. However, a re-dispatch is applied to act against the eventual effects of the worst cases, which have been extracted in the middle maximization level. As noted in Equation (59), the deviation from the power balance condition should be minimized. In addition, the system balance in the worst-case scenario has been expressed by Equation (60). The nodal power balance, considering

both contingency and transmission switching binary variables in the worst-case impact mitigation, is presented in Equation (61). The gas balance under the worst-case scenario with new GFG re-dispatch decision variables could be considered using Equation (62).

$$\Phi = \mathrm{Min} \sum_{t \in \mathrm{T}} \sum_{n \in \Lambda} S_{nt}^+ + S_{nt}^- \tag{59}$$

$$\sum_{i \in \Omega^\mathrm{T}} \Delta p_{i,t}^\mathrm{T} + \sum_{g \in \Omega^\mathrm{G}} \Delta p_{g,t}^\mathrm{G} + \sum_{n \in \Lambda} \left(S_{nt}^+ - S_{nt}^- \right) = \sum_{n \in \Lambda} ND_{n,t} \ \forall t \in \mathrm{T} \tag{60}$$

$$-F_l^{max} a_{lt} y_{lt} \leq \sum_{n \in \Lambda} SF_{n,l} \left(\sum_{i \in \Omega_n^\mathrm{T}} \Delta p_{i,t}^\mathrm{T} + \sum_{g \in \Omega_n^\mathrm{G}} \Delta p_{g,t}^\mathrm{G} + S_{n,t}^+ - S_{n,t}^- - ND_{n,t} \right) \leq a_{lt} y_{lt} F_l^{max} \ \forall l \in NL, t \in \mathrm{T} \tag{61}$$

$$\sum_{j' \in \phi_J(j)} \left(\Delta q_{jj',t}^{out} - \Delta q_{jj',t}^{in} \right) + \sum_{s \in \phi_S(j)} \left(\Delta q_{st}^{out} - \Delta q_{st}^{in} \right) + \sum_{w \in \phi_w(j)} \Delta q_{wt} - \sum_{e \in \phi_e(j)} \Delta q_{et} - \sum_{g \in \phi_{\Omega^\mathrm{G}}(j)} b_g \Delta p_{g,t}^\mathrm{G} = 0 \tag{62}$$

Equations (63)–(71) are recourse counterparts of Equations (34)–(40) and (46)–(49), respectively.

$$q_w^l \leq \Delta q_{wt} \leq q_w^u \tag{63}$$

$$\Delta r_{st} = \Delta r_{s,t-1} + \Delta q_{st}^{in} - \Delta q_{st}^{out} \tag{64}$$

$$r_s^l \leq \Delta r_{st} \leq r_s^u \tag{65}$$

$$0 \leq \Delta q_{st}^{in} \leq q_{s,max}^{in} \tag{66}$$

$$0 \leq \Delta q_{st}^{out} \leq q_{s,max}^{out} \tag{67}$$

$$(\tau_j^l)^2 \leq \Delta v_{jt} \leq (\tau_j^u)^2 \tag{68}$$

$$\Delta q_{yt} |\Delta q_{yt}| = \psi_y (\Delta v_{i1t} - \Delta v_{j2t}) \tag{69}$$

$$\Delta v_{j2} \leq \gamma_c^2 b_c \Delta v_{j1} + (1 - b_c)(\tau_{j2}^u)^2 \tag{70}$$

$$0 \leq \Delta q_{ct} \leq M b_c \tag{71}$$

The lower-level variables could be linked to the predefined decisions found in the previous minimization step based on Equations (72)–(75). The variables for recourse decision making should be limited based on found decisions in the upper optimization problem; output power reserves, capacities, and commitment conditions of units. It is noted that the suffix (*) represents that the term is fixed as a parameter in the current stage. Finally, Equation (76) shows the positive recourse decision variables.

$$\Delta p_{i,t}^\mathrm{T} \leq P_{i,t}^{\mathrm{T}*} + SP_{i,t}^{\mathrm{Tu}*} \quad \forall i \in \Omega^\mathrm{T}, t \in \mathrm{T} \tag{72}$$

$$\Delta p_{i,t}^\mathrm{T} \geq P_{i,t}^{\mathrm{T}*} - SP_{i,t}^{\mathrm{Td}*} \quad \forall i \in \Omega^\mathrm{T}, t \in \mathrm{T} \tag{73}$$

$$\Delta p_{g,t}^\mathrm{G} \leq P_{g,t}^{\mathrm{G}*} + SP_{g,t}^{\mathrm{Gu}*} \quad \forall g \in \Omega^\mathrm{G}, t \in \mathrm{T} \tag{74}$$

$$\Delta p_{g,t}^\mathrm{G} \geq P_{g,t}^{\mathrm{G}*} - SP_{g,t}^{\mathrm{Gu}*} \quad \forall g \in \Omega^\mathrm{G}, t \in \mathrm{T} \tag{75}$$

$$\left\{ \Delta p_{i,t}^\mathrm{T}, \Delta p_{g,t}^\mathrm{G}, S_{n,t}^+, S_{n,t}^- \right\} \geq 0 \Big] \Big\} \tag{76}$$

3.2. Nested CCG

Since the lower level of the proposed optimization problem is a mixed-integer problem, including transmission switching decision variables, as shown in (61), and linearized gas flow using (69), the conventional CCG solution method would not be applicable. Accordingly, the nested CCG [26,34] is implemented according to the nonconvex binary variables at the lower minimization level.

The developed and introduced tri-level robust optimization model can be expressed in a compact form, as demonstrated in Equations (77)–(82):

$$Obj_{upper} = \min_{\mathbf{x},\mathbf{p}} \mathbf{c}_b^{\mathrm{T}}\mathbf{x} + \mathbf{c}_{gen}^{\mathrm{T}}\mathbf{p} \tag{77}$$

$$\text{s.t.} \quad \mathbf{Ax} + \mathbf{Bp} \leq \mathbf{b} \tag{78}$$

$$Obj_{middle} = \max_{\varepsilon \in U} \mathbf{h}^{\mathrm{T}}\mathbf{y} \tag{79}$$

$$\text{s.t.} \quad \mathbf{C}\varepsilon \leq \mathbf{d} \tag{80}$$

$$Obj_{lower} = \min_{\mathbf{y},\mathbf{z}} \mathbf{h}^{\mathrm{T}}\mathbf{y} \tag{81}$$

$$\text{s.t.} \quad \mathbf{E}(\mathbf{x},\mathbf{p},\varepsilon)\mathbf{y} + \mathbf{F}(\mathbf{x},\mathbf{p},\varepsilon)\mathbf{z} \leq \mathbf{j} \tag{82}$$

The interactions between the discussed compact formulation and the extended form of the proposed model are presented in Table 2.

Table 2. Compact forms of the actual model.

Compact Form	Actual Proposed Model
x	x_{it}, x_{gt}, and binary variables of the linearized expression of (41)
p	$p_{i,t}^{\mathrm{Tr}}, p_{g,t}^{\mathrm{G}}, SP_{i,t}^{\mathrm{Tru}}, SP_{i,t}^{\mathrm{Trd}}, SP_{g,t}^{\mathrm{Gu}}, SP_{g,t}^{\mathrm{Gd}}, q_{wt}, r_{st}, q_{st}^{in}, q_{st}^{out}, v_{jt}, q_{et}, q_{yt}, q_{ct}$ and auxiliary continuous variables for the linearized expression of (41)
y	$S_{nt}^{+}, S_{nt}^{-}, \Delta p_{i,t}^{\mathrm{T}}, \Delta p_{g,t}^{\mathrm{G}}, \Delta q_{jj',t}^{out}, \Delta q_{jj',t}^{in}, \Delta q_{st}^{out}, \Delta q_{st}^{in}, \Delta q_{wt}, \Delta q_{et}, \Delta r_{st}, \Delta v_{jt}, \Delta q_{yt}, \Delta q_{ct}$ and auxiliary continuous variables for the linearized expression of (69)
ε	$z_{n,t}^{u+}, z_{n,t}^{u}, z_{n,t}^{u-}, z_{n,t}^{u}, z_{n,t}^{d+}, z_{n,t}^{d}, z_{n,t}^{d-}, z_{n,t}^{d}, U_{n,t}^{+}, U_{n,t}^{-}, D_{n,t}^{+}, D_{n,t}^{-}, a_{lt}$
z	y_{lt}, and auxiliary binary variables regarding the linearized expression of (69)
$\mathbf{c}_b^{\mathrm{T}}\mathbf{x}$	$C_i^{\mathrm{Tr,SU}}, C_g^{\mathrm{G,SU}}, x_{i,t}C_i^{\mathrm{Tr,NL}}, x_{g,t}C_g^{\mathrm{G,NL}}$
$\mathbf{c}_{gen}^{\mathrm{T}}\mathbf{p}$	$c_i^{\mathrm{Tr}}P_{i,t}^{\mathrm{Tr}}, USC_i^{\mathrm{Tr}}SP_{i,t}^{\mathrm{Tru}}, DSC_i^{\mathrm{Tr}}SP_{i,t}^{\mathrm{Trd}}, Q_w q_{wt}, Q_s q_{st}, c_g^{\mathrm{G}}P_{g,t}^{\mathrm{G}}, USC_g^{\mathrm{G}}SP_{g,t}^{\mathrm{Gu}}, DSC_g^{\mathrm{G}}SP_{g,t}^{\mathrm{Gd}}$
(78)	(24) to (53)
(79)	(55)
(80)	(56) to (58)
(81)	(59)
(82)	(60) to (76)

To apply the nested CCG method, it is necessary to define the inner and outer CCG models.

3.2.1. Inner CCG Problem

Step 1

The inner minimization problem will be mixed-integer programming. Hence, an arbitrary set of worst-case variables should be created as initial values to linearize the inner problem. Based on the upper-level variables, as expressed in Equations (81) and (82), it would be a pure convex linear problem, as shown in Equations (83) and (84).

$$\min_{\mathbf{y},\mathbf{z}} \mathbf{h}^{\mathrm{T}}\mathbf{y} \tag{83}$$

$$\text{s.t.} \quad \mathbf{E}(\mathbf{x}*,\mathbf{p}*,\varepsilon*)\mathbf{y} + \mathbf{F}(\mathbf{x}*,\mathbf{p}*,\varepsilon*)\mathbf{z} \leq \mathbf{j} \tag{84}$$

The determined optimum results of $\mathbf{y}*, \mathbf{z}*$, let $LB = \mathbf{h}^{\mathrm{T}}\mathbf{y}*$, $UB = +\infty$, i=1, I = {1}, $\mathbf{z}^1* = \mathbf{z}*$, $Z = \{\mathbf{z}^1*\}$.

Step 2

The inner minimization problem is a convex linear problem based on the upper-level variables $\mathbf{x}*, \mathbf{p}*$, and $\mathbf{z}*$. Additionally, the inner minimization problem's dual can be obtained. The achieved max-max MILP problem, including bilinear terms, and its

linearization could be simplified by the big M approach [35]. Then, the inner max MILP could be solved using Equations (85) and (86).

$$Obj_{middle} = \max_{\eta,\varepsilon,\boldsymbol{\lambda}} \eta \tag{85}$$

$$\text{s.t. } \eta \leq (\mathbf{j} - \mathbf{F}(\mathbf{x}*,\mathbf{p}*,\varepsilon)z*)^{\mathrm{T}}\boldsymbol{\lambda} \quad \mathbf{C}\varepsilon \leq \mathbf{d}, \ E(\mathbf{x}^*,\mathbf{p}^*,\varepsilon)^{\mathrm{T}}\boldsymbol{\lambda} \geq \mathbf{h}^{\mathrm{T}}, \boldsymbol{\lambda} \geq 0 \tag{86}$$

The optimum results $\varepsilon*$ and $\eta*$ should be extracted. Afterward, $UB = \eta*$ is updated.

Step 3

The problem defined in Equations (83) and (84) is solved using $\varepsilon*$ to determine the optimized results $\mathbf{y}*, \mathbf{z}*$ and upgrade $LB = \max\{LB, \mathbf{h}^{\mathrm{T}}\mathbf{y}*\}$.

Step 4

If $UB - LB \leq C_{tol}^{inner}$, where C_{tol} is the inner CCG convergence tolerance, the process is terminated and returned to the optimum extreme points based on the worst conditions $\varepsilon*$. On the other hand, the iteration number (m) is updated, and Step 2 is followed based on Equations (87) and (88).

$$\eta \leq (\mathbf{j} - \mathbf{F}(\mathbf{x}*,\mathbf{p}*,\varepsilon)\mathbf{z}^{m}*)^{\mathrm{T}}\boldsymbol{\lambda}^{m} \quad \forall m \in NM \tag{87}$$

$$E(\mathbf{x}^*,\mathbf{p}^*,\varepsilon)^{\mathrm{T}}\boldsymbol{\lambda}^{m} \geq \mathbf{h}^{\mathrm{T}}, \boldsymbol{\lambda}^{m} \geq 0 \tag{88}$$

3.2.2. Outer CCG Problem

Step 1

The upper level is solved using Equations (89)–(92) based on the returned extreme points $\varepsilon*$.

$$\min_{\mathbf{x},\mathbf{p}} \phi \tag{89}$$

$$\text{s.t. } \mathbf{Ax+Bp} \leq \mathbf{b} \tag{90}$$

$$\phi \leq \mathbf{c}_{b}^{\mathrm{T}}\mathbf{x} + \mathbf{c}_{gen}^{\mathrm{T}}\mathbf{p} + \mathbf{h}^{\mathrm{T}}\mathbf{y}^{\omega} \quad \forall \omega \in \Omega \tag{91}$$

$$\mathbf{E}(\mathbf{x},\mathbf{p},\varepsilon^{\omega}*)\mathbf{y}^{\omega} + \mathbf{F}(\mathbf{x},\mathbf{p},\varepsilon^{\omega}*)\mathbf{z}^{\omega} \leq \mathbf{j} \ \omega \in \Omega \tag{92}$$

In any iteration $\omega \in \Omega$, primal cuts Equations (91) and (92) should be applied to the main problem. The $LB = \min\{UB, \phi*\}$ is updated with the optimal solution $\mathbf{x}*, \mathbf{p}*, \phi*$.

Step 2

By applying the optimal $\mathbf{x}*, \mathbf{p}*$, the first step of the inner level, as shown in Equations (83) and (84), could be solved to determine the extreme optimal points $\varepsilon*$ for the next iteration. Additionally, The $UB = \min\{UB, Obj_{middle}\}$ should be updated.

Step 3

If $UB - LB \leq C_{tol}^{out}$, where C_{tol}^{out} is the outer CCG convergence tolerance, the process is terminated and returned to the optimal solution. Otherwise, the iteration number is updated, and the following primal cuts, as expressed in Equations (93) and (94), are added to Step 1.

$$\phi \leq \mathbf{h}^{\mathrm{T}}\mathbf{y}^{\omega} \quad \forall \omega \in \Omega \tag{93}$$

$$\mathbf{E}(\mathbf{x},\mathbf{p},\varepsilon^{\omega}*)\mathbf{y}^{\omega} + \mathbf{F}(\mathbf{x},\mathbf{p},\varepsilon^{\omega}*)\mathbf{z}^{\omega} \leq \mathbf{j} \ \omega \in \Omega \tag{94}$$

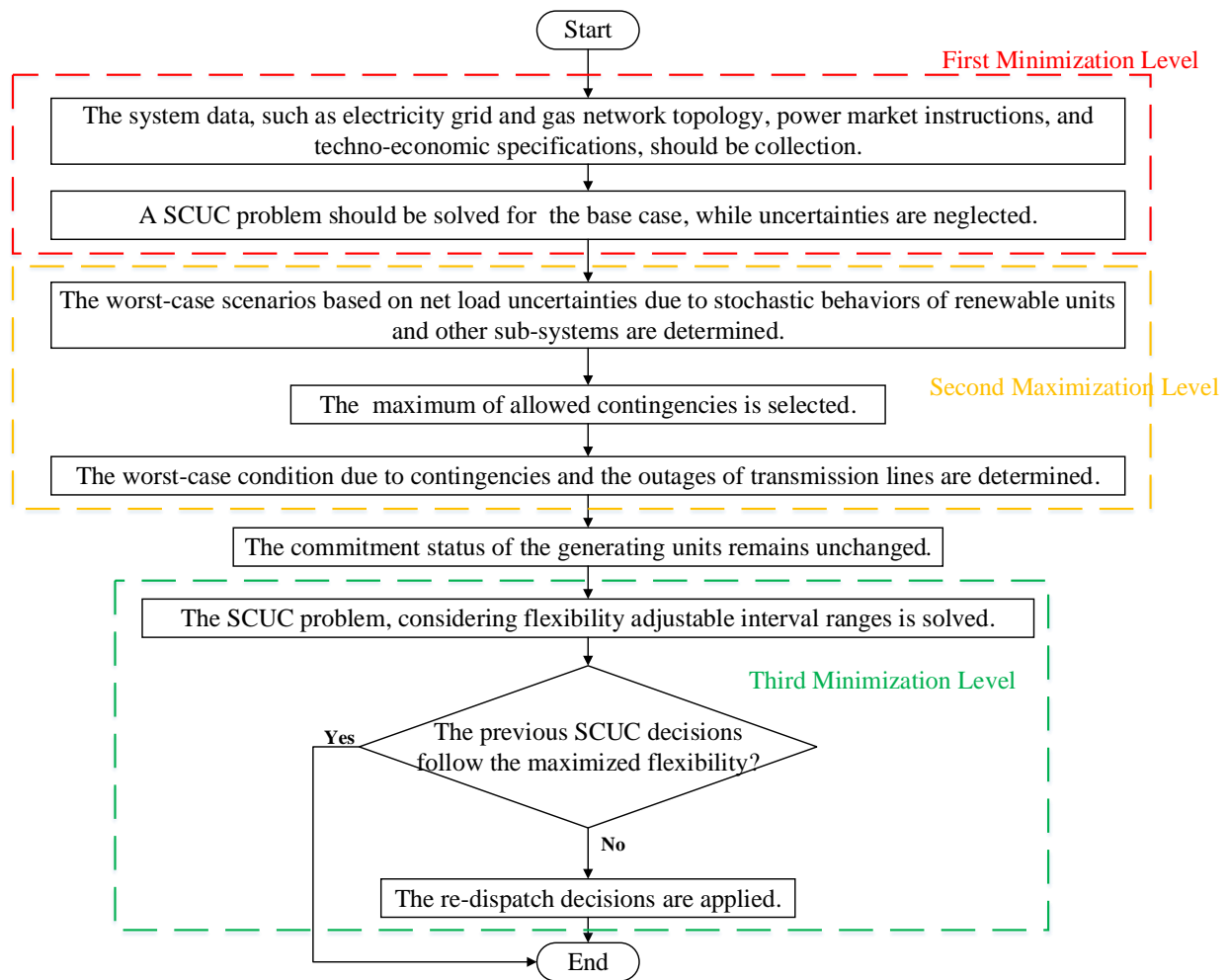Figure 2 shows the flowchart of the solution method.

Figure 2. Flowchart of the proposed method.

4. Numerical Results

In this section, the applicability of the proposed model is tested on two joint electricity and natural gas networks test systems [36,37]:

- Test system 1: A six-bus electrical network incorporating a seven-node gas system, as shown in Figure 3 [36];
- Test system 2: A 39-bus electrical network incorporating a 20-node gas system, as shown in Figure 4 [37].
- The information on the selected hybrid electrical and gas networks has been extracted from [36].
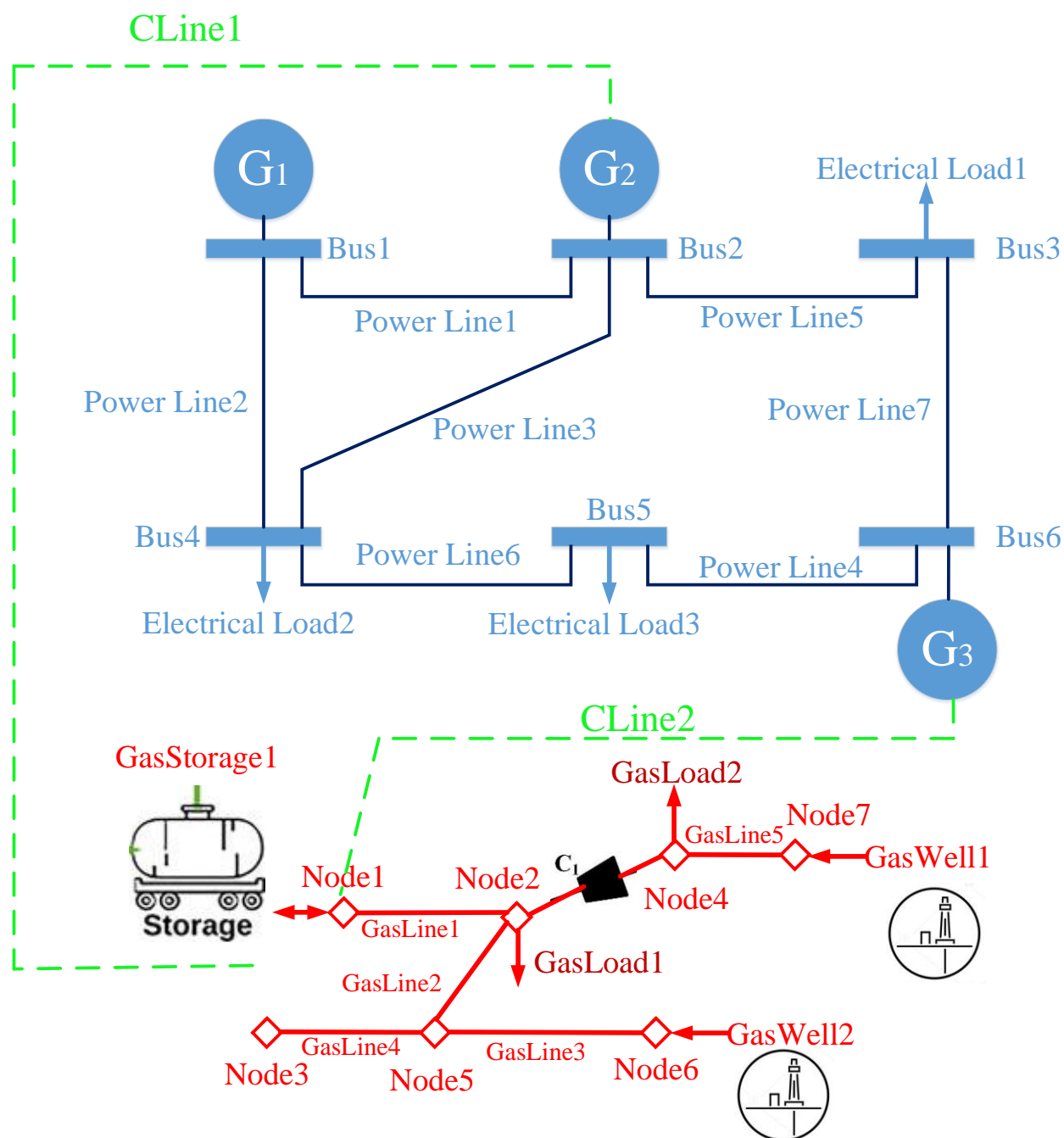
Figure 3. Six-bus power system, incorporating a seven-node gas system [36].
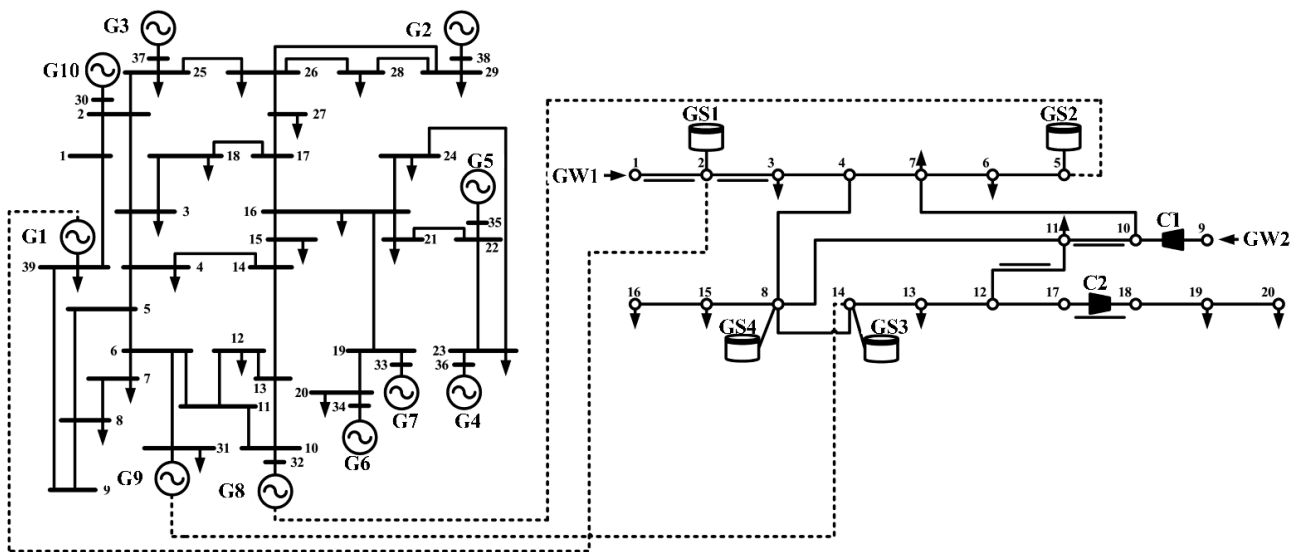
Figure 4. IEEE 39-bus power system, incorporating a 20-node gas system [37].

The degree of robustness is shown in all cases with the normalized budget of uncertainty (NBU). The zero value of the NBU shows the most optimistic results with no uncertainty, and the one value for the NBU represents the most conservative results.

Solving the optimization problems and guaranteeing to find the global optima are essential issues [38–40]. Hence, it was tried to develop effective approaches for solving the optimization problem.

4.1. Test Results of the First Test System

Tables 3 and 4 demonstrates the power flow of this test case in two conditions:

- Base case (without uncertainties)
- The most conservative solution with NBU = 1.0

As highlighted in grey color, the most loaded line for the base case was L1, which was correctly recognized as the worst case in the proposed model, and disconnected for the sake of finding the most reliable operation scheduling with the highest robustness cost. In that case, line L2 was fully loaded to compensate for the failure of line L1. It is worth mentioning that due to the lack of redundant transmission network loops, transmission switching was not activated for this small test case.

Table 5 is provided to briefly demonstrate the out-of-sample results of the proposed model in a long-run simulation through the Monte Carlo simulation. As highlighted in grey color, the lowest total cost belongs to the case with NBU = 0.2. In this risk level, with a rather slight increase (7.3%) in the operation cost (249,953 − 232,782 = 17,171 USD), a large reduction (89%) in the out of sample cost was obtained (375,500 − 41,051 = 334,449 USD). This shows the effectiveness of the proposed model that even small conservative solutions cause large operation reliability enhancement.

Table 3. Power flow comparison for base case.

h	Base Case						
	Line No.						
	L1	L2	L3	L4	L5	L6	L7
1	54	46	14	−5	40	−10	5
2	55	50	19	−13	46	3	13
3	61	56	21	−18	50	14	18
4	60	55	21	−18	49	14	18
5	54	46	14	−8	39	−1	8
6	54	46	14	−8	40	−3	8
7	54	46	14	−6	40	−9	6
8	61	55	20	−13	51	−1	13
9	57	51	18	−8	49	−13	8
10	64	58	20	−1	54	−9	11
11	75	68	24	−15	61	0	15
12	70	62	22	−11	58	−10	11
13	85	76	27	−19	68	7	19
14	78	70	24	−15	63	−3	15
15	102	96	37	−34	84	33	34
16	100	100	44	−43	94	42	43
17	103	100	42	−40	91	39	40
18	96	87	31	−26	75	20	26
19	88	79	28	−21	70	9	21
20	77	69	24	−15	63	−1	15
21	84	76	27	−20	67	8	20
22	74	67	24	−15	61	0	15
23	58	52	18	−9	49	−10	9
24	59	53	19	−10	50	−7	10

Table 4. Power flow comparison robust cases with NBU = 1.0.

	NBU=1.0					
h	**Line No.**					
	L2	**L3**	**L4**	**L5**	**L6**	**L7**
1	100	−15	20	15	14	−20
2	100	− 8	10	23	26	−10
3	100	−3	2	29	34	−2
4	100	−3	3	28	35	−3
5	100	−15	16	15	23	−16
6	100	−15	17	15	21	−17
7	100	−15	19	15	15	−19
8	100	−4	8	30	20	−8
9	100	4	0	41	21	0
10	100	−2	9	35	11	−9
11	100	6	−1	46	15	1
12	100	14	−9	56	20	9
13	100	14	−8	57	17	8
14	100	8	−1	50	11	1
15	100	15	−15	65	52	15
16	100	13	−16	67	69	16
17	100	18	−11	62	15	11
18	100	18	−13	62	19	13
19	100	17	−11	60	18	11
20	100	8	−1	49	13	1
21	100	14	−9	56	19	9
22	100	6	0	45	15	0
23	100	−7	13	27	12	−13
24	100	−6	11	28	15	11

Table 5. Out-of-sample analysis results for various NBUs for the 6-bus test system.

NBU	**Cost (USD)**		
	SCUC	**MCS**	**Total**
0	232,782	375,500	608,282
0.1	243,855	150,002	393,857
0.2 *	249,953	41,051	291,004
0.3	271,222	23,853	295,075
0.4	296,687	1,149	297,836
0.5	337,612	0	337,612
0.6	365,200	0	365,200
0.7	393,152	0	393,152
0.8	420,707	0	420,707
0.9	448,859	0	448,859
1.0	475,553	0	475,553

* The minimum operation cost has appeared corresponding to NBU=0.2, which has been highlighted.

4.2. Test Results of the Second Test System

The results for the IEEE 39-bus system are tabulated in Table 6. To implement the proposed method for this case, a slight modification was done, which was dropping the connecting generator buses to the network, i.e., buses 30, 32, 33, 34, 35, 36, 37, and 38. The rationale behind this was to prevent contingencies in the tie lines connecting the generators

to the network. Without this modification, when NBU equals 1.0, the line connecting buses 38 to 29 that connects G2 to the network was identified as the worst contingency. In addition, disconnecting the G2 caused extra-large load shedding with a total cost of 8,383,356 USD. However, for the same case, by the above-mentioned modification, the total cost of the proposed model was reduced to 1,112,770 USD.

Table 7 briefly shows the results of the proposed model considering TS allowance. It is noted that if TS was not considered, the total cost rose up to 18.8% (1,370,804 USD − 1,112,770 USD = 258,034 USD), which shows the major role of TS in cost reduction in stressed operation conditions. This cost reduction was caused by switching off the connecting line between buses 3 and 4 during almost all of the hours except 1:00, 2:00, 17:00, 23:00, and 24:00. In addition, connecting the line between buses 26 and 27 was identified as the worst contingency in electric transmission lines.

In addition, two gas wells were added in gas nodes 16 and 20 to prevent gas load curtailment in stressed operating conditions. The gas production profile of the gas wells is depicted in Figure 5. It is noted that gas wells w1, w2, w3, and w4 were connected to nodes 1, 9, 16, and 20, respectively. As expected, the least expensive well (w1) produced gas up to its capacity throughout the time horizon, while the more expensive well (w2) produced gas mostly during afternoon peak hours to support electric power flexibility when reserves were scarce. The same trend could be observed in the optimal behavior of gas storage systems, as shown in Figure 6, where storage 2 discharges during daily peak hours between 8:00 and 14:00 with discharges during low-demand hours.

Table 6. Analysis of out-of-sample of various NBUs for the IEEE 39-bus test system with the variable interval range based on the proposed method.

NBU	Cost (USD)		
	SCUC	MCS	Total
0	1,087,471	485,690	1,573,161
0.1	1,089,261	270,550	1,359,811
0.2	1,091,016	239,574	1,330,590
0.3 *	1,094,580	1,542	1,096,122
0.4	1,098,159	0	1,098,159
0.5	1,105,366	0	1,105,366
0.6	1,106,844	0	1,106,844
0.7	1,108,221	0	1,108,321
0.8	1,109,703	0	1,109,703
0.9	1,111,283	0	1,111,283
1.0	1,112,770	0	1,112,770

* The minimum operation cost has appeared corresponding to NBU = 0.3, which has been highlighted.

Table 7. Analysis of out-of-sample of various NBU values for the IEEE 39-bus test system with a fixed interval range.

NBU	Cost (USD)		
	SCUC	MCS	Total
0	1,037,616	776,335	1,813,951
0.1	1,039,324	490,500	1,529,824
0.2	1,040,998	376,310	1,417,308
0.3	1,041,548	210,560	1,252,108
0.4	1,048,028	191,230	1,239,258
0.5	1,054,961	104,097	1,159,058
0.6	1,078,666	56,652	1,135,318
0.7	1,094,159	19,023	1,113,182
0.8 *	1,101,072	0	1,101,072
0.9	1,109,863	0	1,109,863
1.0	1,111,348	0	1,111,348

* The minimum operation cost has appeared corresponding to NBU = 0.3, which has been highlighted.
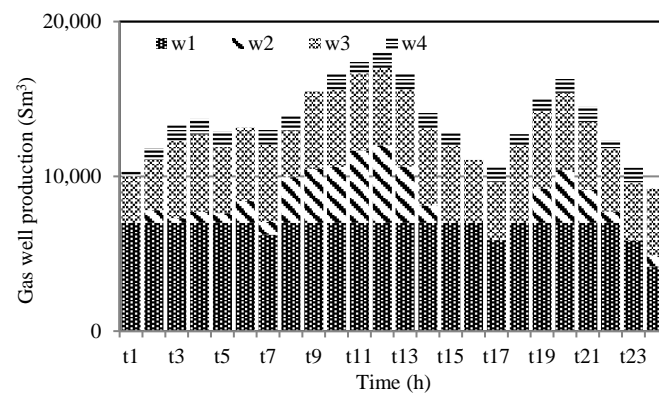
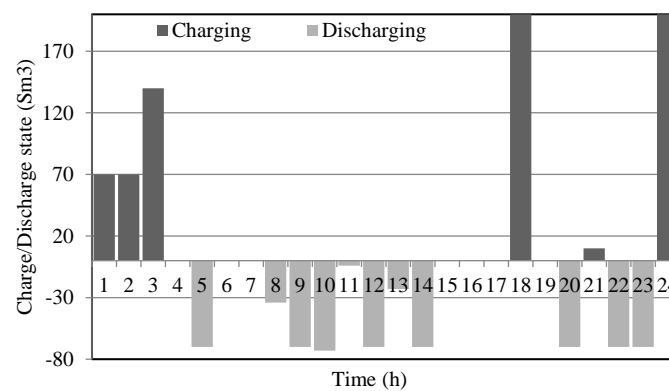**Figure 5.** Gas well production profile for the case NBU = 1.0.

Figure 6. Charging and discharging profile of the second gas storage for NBU = 1.0.

The most important feature of the proposed model is to consider the conventional fixed respective range as an uncertain parameter. Figure 7 shows the performance of this uncertain respective range for the case with NBU = 0.3. As can be seen, for hours 1:00 to 4:00, 12:00 to 17:00, and 21:00 to 24:00, the worst scenario was the lowest wind power production, i.e., Low IR-. However, for the fifth and 12th time periods, the worst-case happened in the upper bound of the positive direction interval range (UP IR+) to force operation scheduling, which was capable of extra ramp ranges compared to the fourth and 13th time periods, respectively. The proposed method considers the flexibility of each time interval and includes the ramping flexibility between consecutive time intervals. Other steep jumps can also be seen in Figure 7 (like 17:00 to 18:00 and 20:00 to 21:00).
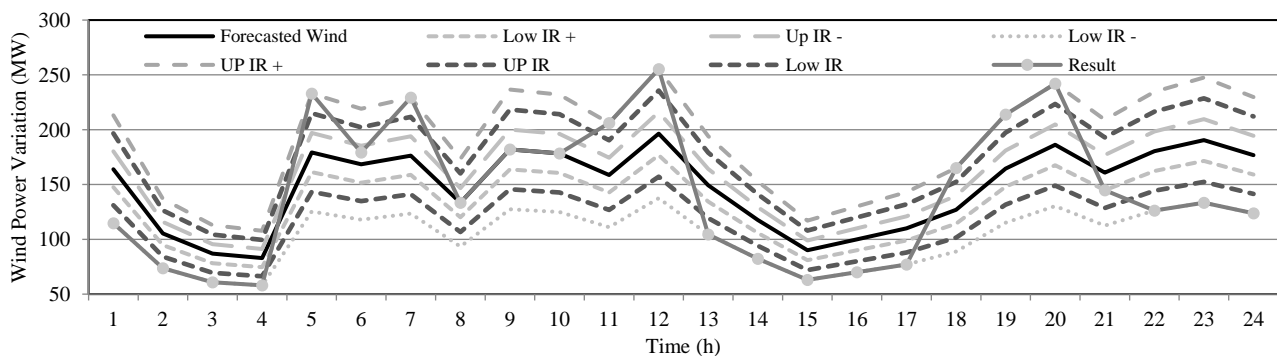

Figure 7. Optimal worst-case for NBU = 0.3 based on uncertain respective range modeling.

As revealed by the test results, the execution time for the studied networks was very short. Therefore, it can be concluded that the proposed method can be practically implemented for large networks.

5. Conclusions

The proposed model tried to solve robust day-ahead scheduling of joint electricity and gas networks based on new features. The first new aspect of the current paper was that fixed respective range (interval range) in conventional robust models was substituted with an uncertain respective range to better mimic the real-world characteristics of uncertain resources, such as wind power generation. In addition, the transmission switching technique was applied in the joint electricity and gas operation problem by virtue of more flexibility. Since the multilevel robust optimization model could not be solved with conventional CCG algorithms because of nonconvexities in the inner minimization problem, a recent nested CCG algorithm was applied to overcome this shortcoming. The results were promising because of electricity networks with a higher number of transmission loops. Hence, the network operator could benefit from transmission line switching even considering the N-1 transmission line security criterion. The tractability of the proposed model could be improved, considering larger electricity and gas networks. The uncertain respective range can be investigated in other power system popular problems, such as security constraint unit commitment and robust economic dispatch. The multiresolution scheduling could also be investigated to capture more variability of the renewables with finer time resolutions. The comparison of two methods based on variable and fixed flexibility interval ranges has emphasized the effectiveness of this study. Furthermore, the operation cost of the study network in NBU=0.8 was obtained to be 1,101,072 USD, but in in NBU = 0.3, the operation cost could be reduced to 1,096,122 USD, which illustrates the advantages of the proposed method.

Author Contributions: Conceptualization, M.G. and H.H.-D.; methodology, M.G., M.A.H. and H.H.-D.; software, M.G. and H.H.-D.; validation, M.G., M.A.H. and H.H.-D.; formal analysis, M.G., M.A.H. and H.H.-D.; investigation, M.G., M.A.H. and H.H.-D.; resources, M.G. and H.H.-D.; data curation, M.G.; writing—original draft preparation, M.G.; writing—review and editing, M.A.H. and H.H.-D.; visualization, M.G., M.A.H. and H.H.-D.; supervision, M.A.H. and H.H.-D.; project administration, M.A.H. and H.H.-D.; funding acquisition, M.A.H. and H.H.-D. All authors have read and agreed to the published version of the manuscript.

Nomenclature

Set and Indices

$t \in T$	Index of time period
$i \in \Omega^{\text{Tr}}$	Index of conventional generator
$g \in \Omega^{\text{G}}$	Index of gas-fired generator (GFG)
$l \in NL$	Index of transmission line in the electricity network
$n \in \Lambda$	Index of bus
$w \in W$	Index of gas well
$s \in S$	Index of gas storage tank
$c \in C$	Index of gas compressor
$j, j' \in J$	Index of the gas network bus
$y \in Y$	Index of the gas network line
$e \in E$	Index of gas load
$\{\cdot\} \in \phi_{\{\cdot\}}(j)$	Subset of components connected to the j-th gas node

Parameters

b_c	Compressor indicator between two gas nodes
b_g	Heat rate coefficient of the g-th GFG [MBTU/MWh]
$C_{g/i}^{\text{G/Tr,NL}}$	No-load cost coefficient of GFGs/thermal generators (TGs)
$C_{g/i}^{\text{G/Tr,SU}}$	Start-up cost of GFGs/TGs
$c_{g/i}^{\text{G/Tr}}$	Operation fuel cost of GFG/TG [USD/MWh]
$\text{DSC}_{g/i}^{\text{G/Tr}}$	Downward reserve price coefficient of GFG/TG [USD/MWh]
$F_l^{\max}$	Thermal limit of the l-th line [MW]
$\text{NL}_{n,t}$	Forecasted net load at the n-th bus and the t-th time
Q_w	Gas price [USD/MBTU]
Q_s	Gas storage price [USD/MBTU]
$P_g^{\text{G,min/max}}$	Lower/upper bounds for the generation capacity of the g-th GFG
$P_i^{\text{Tr,min/max}}$	Minimum/maximum power generation capacity of the i-th TG
$q_w^{l/u}$	Upper and lower bound of gas well production
$q_{s,\max}^{\text{in/out}}$	Maximum limit of inflow/outflow of gas storage
$R_g^{\text{Gu/Gd,max}}$	Up/down reserve capacity bound of the g-th GFG
$R_i^{\text{Tru/Trd,max}}$	Up/down reserve capacity bound of the i-th TG
$r_s^{l/u}$	Lower/Upper limit of the gas storage's state of charge
$SF_{n,l}$	Matrix of shift factor regarding a specified bus and line
$\text{USC}_{g/i}^{\text{G/Tr}}$	Cost of upward reserve procurement of GFG/TG [USD/MWh]
$\text{ND}_{n,t}$	Uncertain net-load at the n-th bus and the t-th time
$L_{n,t}$	Forecasted load at the n-th bus and the t-th time
$\Delta N_{n,t}^{u_0}$	Base net-load variation interval in the upward direction at the n-th bus and the t-th time
$\Delta N_{n,t}^{d_0}$	Base net-load variation interval in the downward direction at the n-th bus and the t-th time
$\Delta N_{n,t}^{u^{+/-}}$	Upward net-load variation interval in positive/negative direction at the n-th bus and the t-th time
$\Delta N_{n,t}^{d^{+/-}}$	Downward net-load variation interval in positive/negative direction at the n-th bus and the t-th time
$\Delta N_{n,t}^{u}$	Uncertain net-load variation interval in the upward direction at the n-th bus and the t-th time
$\Delta N_{n,t}^{d}$	Uncertain net-load variation interval in the downward direction at the n-th bus and the t-th time
$\Gamma, \Gamma^u, \Gamma^d$	Uncertainty's budget for net-load variation/upward and downward respective range deviations at the n-th bus and the t-th time
$\tau_j^{l/u}$	Minimum/maximum pipeline flow limit
ε	Uncertain parameter vector

	Variables	
$P_{g/i,t}^{G/Tr}$	Hourly power generation of GFGs/TGs [MW]	
$S_{nt}^{+/-}$	Variables used in the lower level of the proposed method to capture power imbalances at the n-th bus and the t-th time step	
$q_{w,t}$	Gas production of the w-th well at the t-th time step	
$q_w^{l/u}$	Lower/upper limits of gas well	
$q_{s,t}$	Amount of gas storage of the s-th storage unit at the t-th time	
$q_{s,t}^{in}, q_{s,t}^{out}$	Amount of gas inflow and outflow of the s-th storage unit at the t-th time	
r_{st}	State of charge regarding gas storages	
$SP_{i,t}^{Tru/Trd}$	Upward/downward reserve capacity of TGs	
$SP_{g,t}^{Gu/Gd}$	Upward/downward reserve capacity of GFGs	
$\kappa_{i/g}$	Vector of $x_{g/i,t}$ for all $t \in T$	
$k_{i,g}$	Feasible set for the Minimum up-time and down-time of the i/g-th unit	
Φ^{wc}	The worst-case of the system's power imbalance	
$v_{j,t}$	Volume of gas in the j-th pipeline at the t-th time period	
$x_{g/i,t}$	A binary variable, which is 1 if the GFG/TG is scheduled to be turned on at the t-th time period; otherwise, it would be 0.	
$z_{n,t}^{u/d}$	A binary direction status indicator of net load variation of the n-th node at the t-th time period	
$z_{n,t}^{u+/d+}$	A positive binary direction status indicators of respective range variation of the n-th node at the t-th time period	
$z_{n,t}^{u-/d-}$	A negative binary direction status indicators of respective range variation of the n-th node at the t-th time period	
$U_{n,t}^{+/-}, D_{n,t}^{+/-}$	Auxiliary binary decision variables of the n-th node at the t-th time period	
$\Delta p_{i,t}^{T}, \Delta p_{g,t}^{G}$	Re-dispatch wait and see variable regarding conventional generators and GFGs productions	
$\Delta q_{w,t}$	Re-dispatch wait and see variable regarding gas well productions	
Δr_{st}	Re-dispatch variable regarding the state of charge of gas storage system	
Δq_{st}^{in}	Re-dispatch variable regarding the inflow to the gas storage system	
Δq_{st}^{out}	Re-dispatch variable regarding the outflow of the gas storage system	
Δv_{jt}	Re-dispatch variable regarding the volume of gas in the j-th pipeline	
Δq_c	Re-dispatch variable regarding the gas flow stored in the pipeline	

References

1. Mohammadi, A.; Ashouri, M.; Ahmadi, M.H.; Bidi, M.; Sadeghzadeh, M.; Ming, T. Thermoeconomic analysis and multiobjective optimization of a combined gas turbine, steam, and organic Rankine cycle. *Energy Sci. Eng.* **2018**, *6*, 506–522. [CrossRef]
2. Hajinezhad, A.; Ahmadi, S.S.; Alimoradiyan, H. Feasibility analysis of using novel Sepanta biodiesel fuel as an additive to gas micro-turbine fuels: An experimental study. *Energy Sci. Eng.* **2022**, *10*, 1120–1131. [CrossRef]
3. Guo, H.; Chen, Q.; Xia, Q.; Kang, C. Market equilibrium analysis with high penetration of renewables and gas-fired generation: An empirical case of the Beijing-Tianjin-Tangshan power system. *Appl. Energy* **2018**, *227*, 384–392. [CrossRef]
4. AlHajri, I.; Ahmadian, A.; Elkamel, A. Stochastic day-ahead unit commitment scheduling of integrated electricity and gas networks with hydrogen energy storage (HES), plug-in electric vehicles (PEVs) and renewable energies. *Sustain. Cities Soc.* **2021**, *67*, 102736. [CrossRef]
5. Ahmadi, M.H.; Nazari, M.A.; Ghasempour, R.; Pourfayaz, F.; Rahimzadeh, M.; Ming, T. A review on solar-assisted gas turbines. *Energy Sci. Eng.* **2018**, *6*, 658–674. [CrossRef]
6. Aldarajee, A.H.; Hosseinian, S.H.; Vahidi, B.; Dehghan, S. A coordinated planner-disaster-risk-averse-planner investment model for enhancing the resilience of integrated electric power and natural gas networks. *Int. J. Electr. Power Energy Syst.* **2020**, *119*, 105948. [CrossRef]
7. Li, B.; Roche, R.; Paire, D.; Miraoui, A. Coordinated scheduling of a gas/electricity/heat supply network considering temporal-spatial electric vehicle demands. *Electr. Power Syst. Res.* **2018**, *163*, 382–395. [CrossRef]
8. Chen, Z.; Liu, J.; Liu, X. GPU accelerated power flow calculation of integrated electricity and heat system with component-oriented modeling of district heating network. *Appl. Energy* **2021**, *305*, 117832. [CrossRef]
9. Alabdulwahab, A.; Abusorrah, A.; Zhang, X.; Shahidehpour, M. Stochastic Security-Constrained Scheduling of Coordinated Electricity and Natural Gas Infrastructures. *IEEE Syst. J.* **2015**, *11*, 1674–1683. [CrossRef]
10. Zhao, B.; Lamadrid, A.J.; Blum, R.S.; Kishore, S. A trilevel model against false gas-supply information attacks in electricity systems. *Electr. Power Syst. Res.* **2020**, *189*, 106541. [CrossRef]

11. O'Malley, C.; Delikaraoglou, S.; Roald, L.; Hug, G. Natural gas system dispatch accounting for electricity side flexibility. *Electr. Power Syst. Res.* **2019**, *178*, 106038. [CrossRef]

12. Yang, B. Multi-objective optimization of integrated gas–electricity energy system based on improved multi-object cuckoo algorithm. *Energy Sci. Eng.* **2021**, *9*, 1839–1857. [CrossRef]

13. Ji, Z.; Huang, X. Day-Ahead Schedule and Equilibrium for the Coupled Electricity and Natural Gas Markets. *IEEE Access* **2018**, *6*, 27530–27540. [CrossRef]

14. Chen, R.; Wang, J.; Sun, H. Clearing and Pricing for Coordinated Gas and Electricity Day-Ahead Markets Considering Wind Power Uncertainty. *IEEE Trans. Power Syst.* **2017**, *33*, 2496–2508. [CrossRef]

15. He, Y.; Shahidehpour, M.; Li, Z.; Guo, C.; Zhu, B. Robust Constrained Operation of Integrated Electricity-Natural Gas System Considering Distributed Natural Gas Storage. *IEEE Trans. Sustain. Energy* **2017**, *9*, 1061–1071. [CrossRef]

16. He, C.; Zhang, X.; Liu, T.; Wu, L. Distributionally Robust Scheduling of Integrated Gas-Electricity Systems With Demand Response. *IEEE Trans. Power Syst.* **2019**, *34*, 3791–3803. [CrossRef]

17. He, Y.; Yan, M.; Shahidehpour, M.; Li, Z.; Guo, C.; Wu, L.; Ding, Y. Decentralized Optimization of Multi-Area Electricity-Natural Gas Flows Based on Cone Reformulation. *IEEE Trans. Power Syst.* **2017**, *33*, 4531–4542. [CrossRef]

18. Khani, H.; Farag, H.E.Z. Optimal Day-Ahead Scheduling of Power-to-Gas Energy Storage and Gas Load Management in Wholesale Electricity and Gas Markets. *IEEE Trans. Sustain. Energy* **2017**, *9*, 940–951. [CrossRef]

19. Chen, J.; Zhang, W.; Zhang, Y.; Bao, G. Day-Ahead Scheduling of Distribution Level Integrated Electricity and Natural Gas System Based on Fast-ADMM With Restart Algorithm. *IEEE Access* **2018**, *6*, 17557–17569. [CrossRef]

20. Nikoobakht, A.; Aghaei, J.; Niknam, T.; Farahmand, H.; Korpås, M. Electric vehicle mobility and optimal grid reconfiguration as flexibility tools in wind integrated power systems. *Int. J. Electr. Power Energy Syst.* **2019**, *110*, 83–94. [CrossRef]

21. Aghaei, J.; Nikoobakht, A.; Mardaneh, M.; Shafie-Khah, M.; Catalão, J.P. Transmission switching, demand response and energy storage systems in an innovative integrated scheme for managing the uncertainty of wind power generation. *Int. J. Electr. Power Energy Syst.* **2018**, *98*, 72–84. [CrossRef]

22. Ding, T.; Zhao, C. Robust optimal transmission switching with the consideration of corrective actions for N—k contingencies. *IET Gener. Transm. Distrib.* **2016**, *10*, 3288–3295. [CrossRef]

23. Saavedra, R.; Street, A.; Arroyo, J.M. Day-Ahead Contingency-Constrained Unit Commitment With Co-Optimized Post-Contingency Transmission Switching. *IEEE Trans. Power Syst.* **2020**, *35*, 4408–4420. [CrossRef]

24. He, C.; Dai, C.; Wu, L.; Liu, T. Robust Network Hardening Strategy for Enhancing Resilience of Integrated Electricity and Natural Gas Distribution Systems Against Natural Disasters. *IEEE Trans. Power Syst.* **2018**, *33*, 5787–5798. [CrossRef]

25. Wang, C.; Wei, W.; Wang, J.; Liu, F.; Mei, S. Strategic Offering and Equilibrium in Coupled Gas and Electricity Markets. *IEEE Trans. Power Syst.* **2017**, *33*, 290–306. [CrossRef]

26. Cobos, N.G.; Arroyo, J.M.; Alguacil-Conde, N.; Wang, J. Robust Energy and Reserve Scheduling Considering Bulk Energy Storage Units and Wind Uncertainty. *IEEE Trans. Power Syst.* **2018**, *33*, 5206–5216. [CrossRef]

27. Luo, F.; Zhang, T.; Wei, W.; Li, F.; Bai, L.; Tan, C.-W.; Liu, Y.; Liu, G. Models and methods for low-carbon footprint analysis of grid-connected photovoltaic generation from a distribution network planning perspective. *Energy Sci. Eng.* **2017**, *5*, 290–301. [CrossRef]

28. Bai, Y.; Wu, X.; Xia, A. An enhanced multi-objective differential evolution algorithm for dynamic environmental economic dispatch of power system with wind power. *Energy Sci. Eng.* **2020**, *9*, 316–329. [CrossRef]

29. Petkovic, M.; Koch, T.; Zittel, J. Deep learning for spatio-temporal supply and demand forecasting in natural gas transmission networks. *Energy Sci. Eng.* **2021**, *10*, 1812–1825. [CrossRef]

30. He, C.; Wu, L.; Liu, T.; Wei, W.; Wang, C. Co-optimization scheduling of interdependent power and gas systems with electricity and gas uncertainties. *Energy* **2018**, *159*, 1003–1015. [CrossRef]

31. Sayed, A.R.; Wang, C.; Chen, S.; Shang, C.; Bi, T. Distributionally robust day-ahead operation of power systems with two-stage gas contracting. *Energy* **2021**, *231*, 120840. [CrossRef]

32. Carrion, M.; Arroyo, J. A Computationally Efficient Mixed-Integer Linear Formulation for the Thermal Unit Commitment Problem. *IEEE Trans. Power Syst.* **2006**, *21*, 1371–1378. [CrossRef]

33. Alizadeh, M.I.; Moghaddam, M.P.; Amjady, N. Multistage Multiresolution Robust Unit Commitment With Nondeterministic Flexible Ramp Considering Load and Wind Variabilities. *IEEE Trans. Sustain. Energy* **2017**, *9*, 872–883. [CrossRef]

34. Cobos, N.G.; Arroyo, J.M.; Alguacil-Conde, N.; Street, A. Robust Energy and Reserve Scheduling Under Wind Uncertainty Considering Fast-Acting Generators. *IEEE Trans. Sustain. Energy* **2018**, *10*, 2142–2151. [CrossRef]

35. Alizadeh, M.; Moghaddam, M.P.; Amjady, N. Flexibility contribution of heat ventilation and air conditioning loads in a multi-stage robust unit commitment with non-deterministic variability-oriented ramp reserves. *IET Gener. Transm. Distrib.* **2018**, *12*, 3037–3045. [CrossRef]

36. Wang, C.; Wei, W.; Wang, J.; Liu, F.; Qiu, F.; Correa-Posada, C.M.; Mei, S. Robust Defense Strategy for Gas–Electric Systems Against Malicious Attacks. *IEEE Trans. Power Syst.* **2016**, *32*, 2953–2965. [CrossRef]

37. Jiang, T.; Northeast Electric Power University; Deng, H.; Bai, L.; Zhang, R.; Li, X.; Chen, H. Optimal energy flow and nodal energy pricing in carbon emission-embedded integrated energy systems. *CSEE J. Power Energy Syst.* **2018**, *4*, 179–187. [CrossRef]

38. Orosz, T.; Rassõlkin, A.; Kallaste, A.; Arsénio, P.; Pánek, D.; Kaska, J.; Karban, P. Robust Design Optimization and Emerging Technologies for Electrical Machines: Challenges and Open Problems. *Appl. Sci.* **2020**, *10*, 6653. [CrossRef]

39. Azari, M.; Mazlumi, K.; Ojaghi, M. Optimal Directional Overcurrent Relay Coordination in Interconnected Networks Considering User-Defined PWL Characteristic Curve. *Arab. J. Sci. Eng.* **2021**, *47*, 3119–3139. [CrossRef]
40. Orosz, T.; Sleisz, A.; Tamus, Z.A. Metaheuristic Optimization Preliminary Design Process of Core-Form Autotransformers. *IEEE Trans. Magn.* **2015**, *52*, 1–10. [CrossRef]